*J. Plasma Physics* (2003), *vol.* 69, *part* 2, *pp.* 93–108.  
DOI: 10.1017/S0022377803002101 Printed in the United Kingdom

# Phase space holes in non-periodic plasmas

ERIC FIJALKOW[1] and LUIGI NOCERA[2]

[1]MAPMO–CNRS-Université d'Orléans, BP 6759, F-45067 Orléans Cedex 2, France
[2]IFAM–CNR, via Moruzzi 1, I-56124 Pisa, Italy
(nocera@ifam.pi.cnr.it)

(Received 25 March 2002 and in revised form 30 September 2002)

**Abstract.** We study the dynamics of phase space holes in a non-collisional plasma by numerical integration of the one-dimensional Vlasov equation. The plasma is bounded and connected to vacuum by two interfaces, which gives rise to *non-periodic boundary conditions*. By choosing different initial conditions, we consider four different situations: development of a sinusoidal wave, two-stream instability, development of an *ab initio* Bernstein–Greene–Kruskal state and the expansion of a plasma into vacuum. For the latter situation ions move with a realistic mass of 1837 electron masses. The most prominent results of our investigation are: (a) a clockwise revolution of holes in phase space; (b) the appearance of stable oscillations of the total electron momentum, which, despite their striking linearity, cannot be related to electrostatic plasma oscillations. To the best of our knowledge none of these phenomena have been reported in kinetic simulations before: indeed we prove that the non-periodicity of the boundary conditions is an *essential* requirement for the sustainment of both hole revolution and momentum oscillations.

## 1. Introduction

Particle depletions in the phase space of a non-collisional plasma (phase space holes) are associated with several prominent nonlinear phenomena in plasmas, such as the asymptotic development of Landau damping (Manfredi 1997), the appearance of Bernstein–Greene–Kruskal (BGK) states (Brunetti et al. 2000), electrostatic echoes (Nocera and Mangeney 1999), solitons (Saeki and Genma 1998; Muschietti et al. 1999) and non-monotonic double layers (Hasegawa and Sato 1982; Han and Kim 1995).

Beside very instructive analytical investigations into the nature and formation mechanisms of phase space holes (Bernstein 1958; Boutros-Ghali and Dupree 1981; Dupree 1982; Schamel 1982, 1986, 2000; Chanteur and Raadu 1987; Terry et al. 1990; Korn and Schamel 1996), the study of phase space holes by numerical solution of Vlasov's equation was also considered. This has indeed been attempted by most diverse numerical approaches, including particle-in-cell (Sato and Okuda 1980; Berman et al. 1986; Han and Kim 1995; Muschietti et al. 1999), waterbag (Berk and Roberts 1967; Roberts and Berk 1967), splitting (Berk et al. 1970; Bertrand et al. 1989; Mineau 1989; Ghizzo et al. 1998; Fijalkow 1999), Fourier–Fourier (Klimas and Farrell 1994) and Fourier–Hermite (Armstrong and Montgomery 1969) algorithms.

With the exception of the particle-in-cell simulation by Muschietti et al. (1999), who applied permeable boundaries with outgoing particle removal, these works used

spatially periodic boundary conditions, in one or possibly two (Fijalkow 1999) and three (Singh et al. 2000; Oppenheim et al. 2001) spatial coordinates.

In this paper we relinquish the assumption of periodicity and consider an ion and electron plasma in a *non-periodic* configuration, which we simulate by a splitting-type code. In such a situation, by suitably choosing the initial conditions, we investigate the development of phase space holes in four different situations: (a) development of a sinusoidal wave, leading to the appearance of non-vanishing mean velocity holes; (b) a two-stream unstable configuration, developing into BGK holes; (c) initially static BGK states, coalescing into a single hole; (d) free expansion of a plasma into vacuum, leading to the appearance of irregularly shaped holes. In cases (a)–(c) ions are immobile, whereas in case (d) they move with a realistic mass of 1837 electron masses.

In all the problems we study, holes appear. However, their behaviour is not the same as in the case of periodic boundary conditions, the most prominent difference being for cases (a)–(c): the direct effect of the non-periodic boundary conditions is prevention of the rectilinear, bulk translational motion of the holes in space, which is so much the hallmark of the periodic situation: rather, in phase space, a central, large, vanishing velocity hole is surrounded by a chain of smaller holes which *periodically revolve* around the main hole in a *clockwise* direction.

Superimposed on such a revolution, a strikingly regular harmonic oscillation of the total electron momentum sets in, no matter how large the amplitude of oscillation. In cases (a) and (c) this oscillation is apparently undamped over very long time-scales and therefore it bears no relation to the plasma oscillations predicted by the standard linear treatment of Vlasov's equation. In case (d) the oscillation is attenuated in time, but its frequency and damping rate are different from Landau's rate. Since these oscillations are very important for the stability of holes, we shall devote part of the paper to the understanding of their attenuation in our otherwise conservative system.

This article is organized as follows. In Sec. 2 we present the basic equations, boundary conditions and the code used for the simulations; cases (a), (b)–(c) and (d) are dealt with in Secs 3–5, respectively; momentum oscillations are analysed in Sec. 6; conclusions are drawn in Sec. 7.

## 2. Numerical code, basic equations and boundary conditions

In the following we solve the Vlasov–Poisson system of equations for a distribution $f_e(x, v_e, t)$ of electrons of charge $-|e|$ and mass $m_e$, moving in a background of fixed, but *inhomogeneously distributed* ions of charge $|e|$:

$$\left.\begin{aligned} &\frac{\partial f_e}{\partial t} + v_e \frac{\partial f_e}{\partial x} - E \frac{\partial f_e}{\partial v_e} = 0, \\ &\frac{\partial E}{\partial x} = n_i - \int_{-\infty}^{\infty} f_e \, dv_e. \end{aligned}\right\} \tag{2.1}$$

Here and in the following time $t$ is normalized to the inverse of the electron plasma frequency $\omega_p = (4\pi n_0 e^2/m_e)^{1/2}$, frequencies to $\omega_p$, velocity $v_e$ to the electrons' thermal speed $v_{Te} = [T_e/m_e]^{1/2}$, the space coordinate $x$ to the Debye length $\lambda_D = v_{Te}/\omega_p$, the electrostatic field $E(x,t)$ to $E_0 = 4\pi(n_0\lambda_D^3)e/\lambda_D^2$, where $T_e$ is the homogeneous electron temperature. The inhomogeneous ion density $n_i(x)$ takes

https://doi.org/10.1017/S0022377803002101 Published online by Cambridge University Press

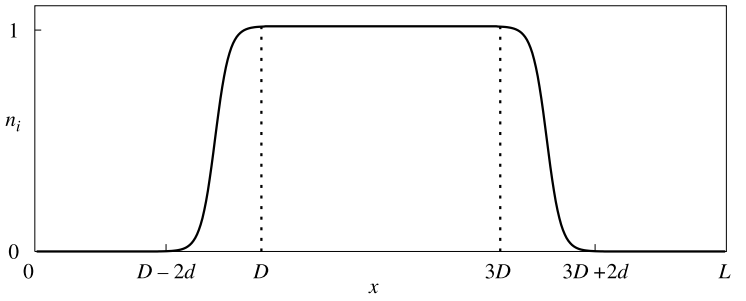


**Figure 1.** The ion density profile of (2.2) used in Figs 2, 3 and 5.

a constant value $n_0$ over the central part of the plasma (the 'plateau') of extent $2D$ and it is connected to vacuum by two interfaces of width $2d$ through Epstein profiles (cf. Fig. 1):

$$n_i(x) = n_0 \begin{cases} 0 & \text{for} \quad 0 \leqslant x < D-2d \\ \frac{1}{2}\{1+\tanh(4[(x-D)/d+1])\} & \text{for} \quad D-2d \leqslant x \leqslant D \\ 1 & \text{for} \quad D < x < 3D \\ \frac{1}{2}\{1+\tanh(4[(x-3D)/d-1])\} & \text{for} \quad 3D \leqslant x \leqslant 3D+2d \\ 0 & \text{for} \quad 3D+2d < x \leqslant L. \end{cases} \tag{2.2}$$

We prescribe the following boundary conditions:

$$f_e(x=0, v_e, t) = f_e(x=L, v_e, t) = 0; \tag{2.3}$$

we choose the $x$-width of the computational box $L$ to be much larger than the extent of the plateau, so that possible 'end effects', induced during the simulations, would have as small a consequence as possible.

We set $d = 120\Delta x$ for the half-width of the interface, where $\Delta x = L/N_x$ is the size of the mesh: this provides a reasonably well-resolved transition between the plasma and vacuum. The extent of the electron velocity space is $-v_{\max e} \leqslant v_e \leqslant -v_{\max e}$. The values of $L, v_{\max e}$ and of the number of points used in the discretization of the $x$ coordinate ($N_x$) and of the velocity coordinate ($N_v$) will be specified in each of the simulations below.

The code used for our numerical computations is basically the 'splitting' code by Shoucri and Gagne (1978), where the periodic splines are, however, changed to *open splines*: this allows us to represent our open system which has no plasma outside the computational box (cf. 2.3). This code turns out to be very suitable for our purposes: a comparatively large time step $\Delta t = 0.1$ ensures a good convergence and stability in all of the following simulations.

## 3. Non-vanishing mean velocity holes

The first instance of our investigation will be to produce 'non-vanishing mean velocity' holes, i.e. holes for which the centre is located in phase space at some positive or negative, non-vanishing velocity coordinate. For this purpose the initial

https://doi.org/10.1017/S0022377803002101 Published online by Cambridge University Press

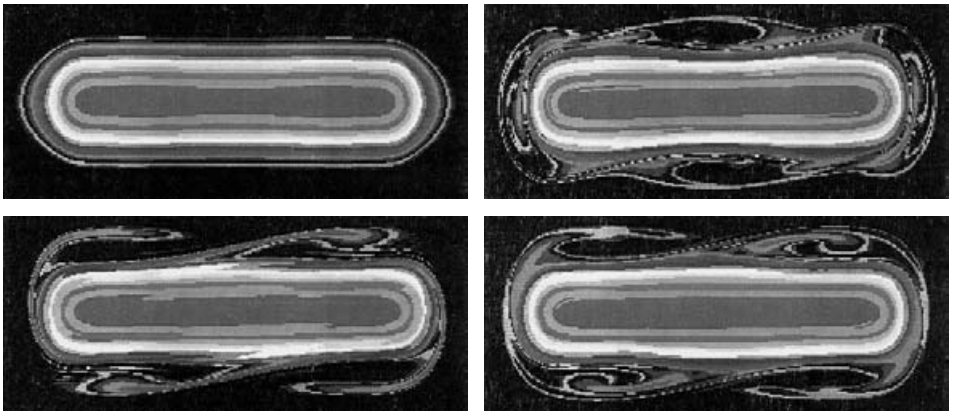

**Figure 2.** Evolution of the electron distribution function for the initial condition in (3.1) (a Maxwellian with a sinusoidal wave perturbation), where $k_0 = 0.3$, $L = 8\pi/k_0$, $\varepsilon = 0.1$, $\alpha = 1$. $N_x = 512, N_v = 320$ points were used. Left-hand column, downward: $t = 0, 30$; right-hand column, downward $t = 66, 96$. In all frames, only a restricted, central part of the phase space is shown: $\frac{1}{8} \leqslant x/L \leqslant \frac{7}{8}, -\frac{1}{2} \leqslant v_e/v_{\max e} \leqslant \frac{1}{2}$.

condition for (2.1) is taken as follows:

$$f_e(x, v_e, t = 0) = n_i(x) h_v(v_e)[1 + \varepsilon \cos(\alpha k_0 x)], \tag{3.1}$$

where

$$h_v(v) = \frac{1}{\sqrt{2\pi}} \exp(-v^2/2), \tag{3.2}$$

$\varepsilon$ is a perturbation amplitude and $2\alpha$ is an integer. Here and in the following sections the fundamental wavenumber will be defined as $k_0 = 2\pi/D$: in this way a wave with mode number $2\alpha$ is excited, having exactly $2\alpha$ maxima within the plateau $D \leqslant x \leqslant 3D$, which vanishes outside the plasma.

In the simulations reported in Fig. 2, we use $k_0 = 0.3$, $D = 2\pi/k_0$, $L = 4D$, $v_{\max e} = 15$, $\varepsilon = 0.1$, $\alpha = 1$, $N_x = 512$, $N_v = 320$. In these conditions only mode number 2 is excited. In the periodic case, this mode would Landau-damp away and four holes moving parallel to the $x$-axis would be created at large times: two of them are positive mean velocity holes and the other two, with the same amplitude, negative mean velocity holes. In the non-periodic case, however, these holes move in phase space in a direction that is not necessarily parallel to the space coordinate and, in fact, *rotates clockwise* around the central part of the phase space (cf. Fig. 2).

To better study the time development of the electron momentum, we perform a second simulation with $\alpha = \frac{3}{2}$ in (3.1): six holes now appear in both the periodic and non-periodic system, as compared in Fig. 3. Hole generation turns out to be a bit faster in the periodic system (cf. Fig. 3 at $t = 30$).

This simulation allows us to uncover a very important difference between the periodic and the non-periodic system, i.e. the behaviour of the total electron momentum

$$P_x = \int_0^L \int_{-\infty}^{\infty} v_e f_e(x, v_e, t)\, dv_e\, dx. \tag{3.3}$$

https://doi.org/10.1017/S0022377803002101 Published online by Cambridge University Press

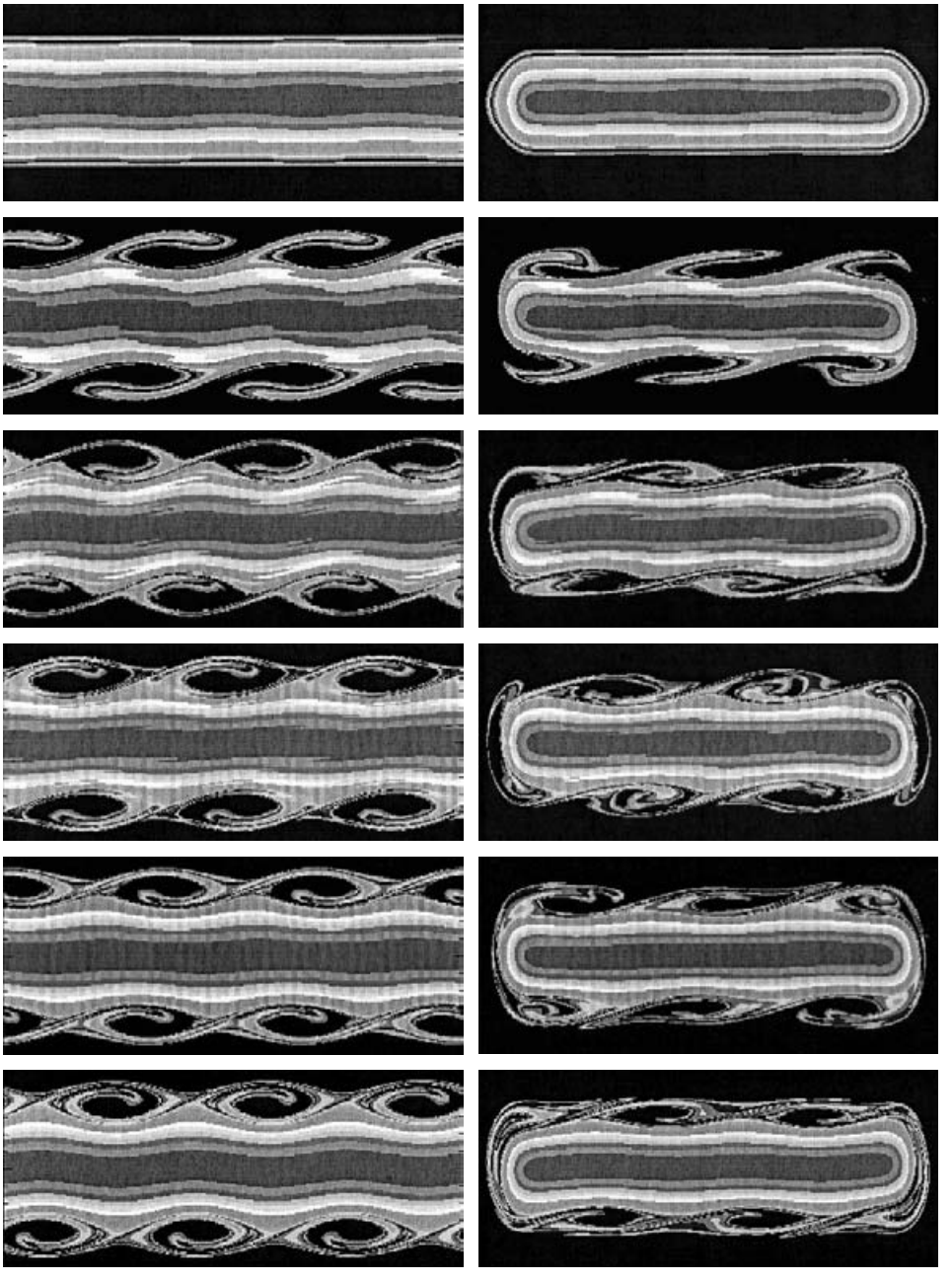

**Figure 3.** Evolution of the electron distribution function for the initial condition in (3.1) (a Maxwellian with a sinusoidal wave perturbation) where $k_0 = 0.3$, $L = 8\pi/k_0$, $\varepsilon = 0.1$, $\alpha = \frac{3}{2}$. $N_x = 512, N_v = 320$ points were used. Comparison between the periodic case (left) and the non-periodic case is shown. Frame pairs, downward: $t = 0, 20, 40, 60, 100, 120$. Only a restricted, central part of the phase space is shown: $\frac{1}{8} \leqslant x/L \leqslant \frac{7}{8}, -\frac{1}{2} \leqslant v_e/v_{\max e} \leqslant \frac{1}{2}$.

https://doi.org/10.1017/S0022377803002101 Published online by Cambridge University Press

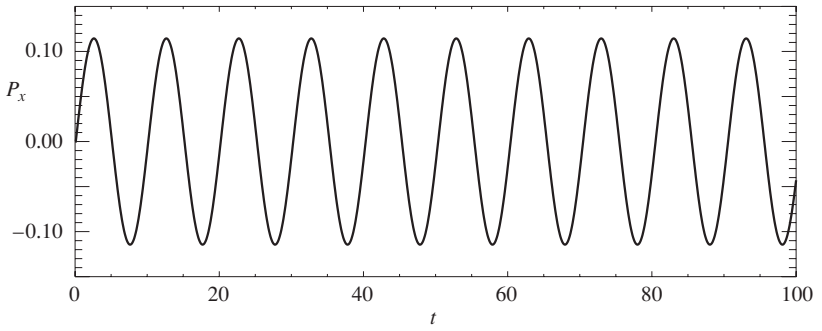


**Figure 4.** Oscillation of the total electron momentum in (3.3) during the development of phase space holes in Fig. 3.

In a periodic system $P_x$ is identically zero. In the non-periodic system, however, $P_x$ *oscillates in time*, apparently undamped, with a period $T \simeq 10$ (cf. Fig. 4). Similar oscillations also exist for smaller values of the perturbation amplitude $\varepsilon$: generally speaking, the smaller this amplitude, the further in the wings of the distribution function (larger $v_e$) holes will appear.

## 4. Holes of the BGK type

To study the evolution of holes with a vanishing mean velocity two possibilities exist: a 'two-stream' initial condition, with a perturbation exciting mode number $n$ (so as to obtain $2n$ holes) and *ab initio* created holes. We shall test both of these possibilities.

For the two-stream case the initial distribution function for electrons streaming at a speed $\pm v_0$ relative to the ions takes the form

$$f_e(x, v_e, t = 0) = \frac{1}{\sqrt{2\pi}} n_i(x) \exp[-(|v_e| - v_0)^2/2][1 + \varepsilon \cos(\alpha k_0 x)]. \tag{4.1}$$

We recall that, in the periodic case, such an initial condition generates a simple equilibrium of the BKG type with two holes: these holes have a vanishing mean velocity and the total momentum $P_x$ in (3.3) is again zero.

In the non-periodic simulations reported in Fig. 5, we use $k_0 = 0.427\,12$, $D = 2\pi/k_0 = 14.7106$, $L = 4D, v_0 = 2, \varepsilon = 0.01, \alpha = 1, N_x = 512, N_v = 320$. We observe the development of the same BGK holes, their mixing and finally their collapse, as indeed in the periodic case (Ghizzo et al. 1998). The difference comes from the appearance of six *non-vanishing mean velocity holes*. These holes rotate around the central vanishing mean velocity hole, as in the case reported in Sec. 3. Also we note the oscillation of the total momentum $P_x$, with the same frequency as in Sec. 3 and a slightly different amplitude (0.175 instead of 0.115).

To study an *ab initio* BGK case, we start with the initial condition (which reduces to the one used by Ghizzo et al. (1988) for $n_i = 1$)

$$f_e(x, v_e, t = 0) = \frac{2\mu}{\sqrt{2\pi}} n_i \left(\frac{1-\zeta}{3-2\zeta}\right) \left(1 + \frac{w_e}{1-\zeta}\right) \exp(-w_e), \tag{4.2}$$

https://doi.org/10.1017/S0022377803002101 Published online by Cambridge University Press

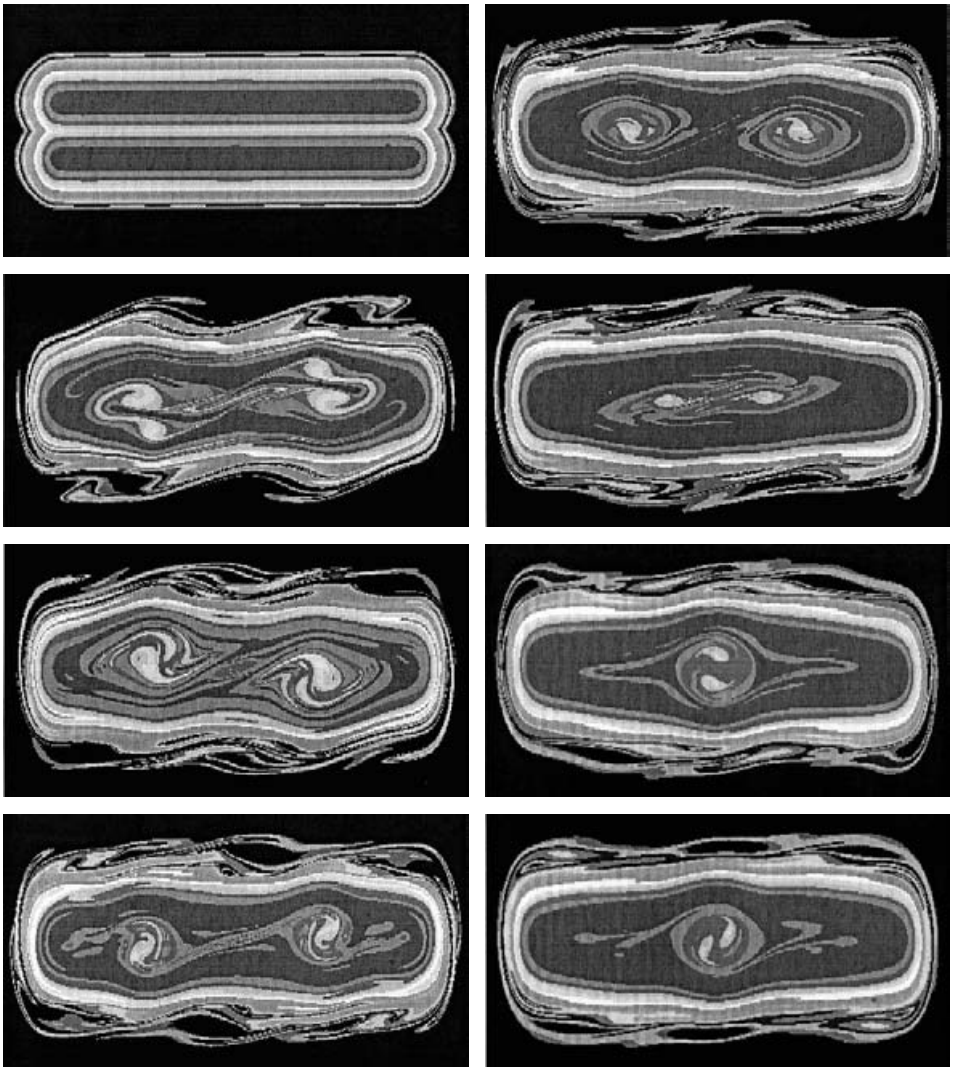

**Figure 5.** Evolution of the electron distribution function for the initial condition in (4.1) (a Maxwellian with a two-stream perturbation), where $k_0 = 0.427\,12$, $L = 8\pi/k_0$, $v_0 = 2$, $\varepsilon = 0.01$, $\alpha = 1$. $N_x = 512$, $N_v = 320$ points were used. Notice the appearance of holes with a zero mean velocity, their collapse and the development of holes with a non-vanishing mean velocity. Left-hand column, downward: $t = 0, 40, 80, 120$; right-hand column, downward: $t = 160, 200, 240, 280$. In all frames, only a restricted, central part of the phase space is shown: $\frac{1}{8} \leqslant x/L \leqslant \frac{7}{8}, -\frac{1}{2} \leqslant v_e/v_{\max e} \leqslant \frac{1}{2}$.

where $w_e$ is the total energy of the electron in the electrostatic potential $\phi(x)$:

$$\left.\begin{aligned} w_e &= v_e^2/2 - \phi(x), \\ \phi(x) &= \begin{cases} \varepsilon \sin(\alpha k_0 x) & \text{for } |x - 2D| < D \\ 0 & \text{for } |x - 2D| \geqslant D. \end{cases} \end{aligned}\right\} \tag{4.3}$$

For the simulations reported in Fig. 6, we choose $k_0 = 0.427\,12, D = 2\pi/k_0 = 14.7106, L = 4D, \mu = 0.92, \zeta = 0.9, \varepsilon = 0.001, \alpha = 1, N_x = 512, N_v = 320$, so that,

https://doi.org/10.1017/S0022377803002101 Published online by Cambridge University Press

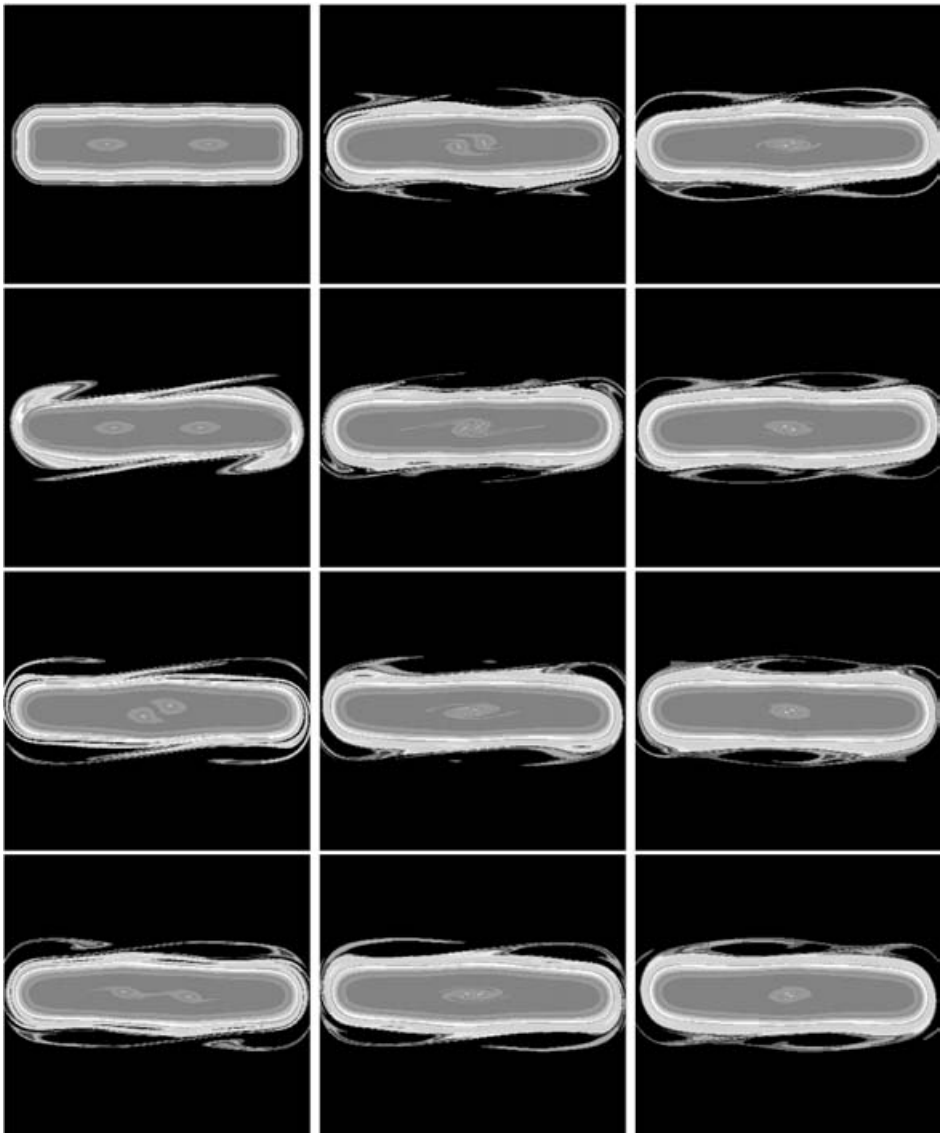

**Figure 6.** Evolution of the electron distribution function for the initial condition in (4.2) and (4.3) (an *ab initio* BGK state), where $k_0 = 0.427\,12, L = 8\pi/k_0$, $\mu = 0.92$, $\zeta = 0.9$, $\varepsilon = 0.001$, $\alpha = 1$. $N_x = 512$, $N_v = 320$ points were used. Notice the merging of the holes into a single hole and the appearance of a non-vanishing velocity hole. Left-hand column, downward: $t = 0, 20, 40, 60$; mid column, downward: $t = 80, 100, 120, 140$; right-hand column, downward: $t = 160, 180, 200, 220$. In all frames, only a restricted, central part of the phase space is shown: $\frac{1}{8} \leqslant x/L \leqslant \frac{7}{8}, -1 \leqslant v_e/v_{\max e} \leqslant 1$.

at $t = 0$, we have two vanishing mean velocity holes. After a short time ($t = 20$), four *non-vanishing mean velocity* holes appear and the classical behaviour of the BGK holes, i.e. coalescence of the two vanishing mean velocity holes into one single hole, sets in. As in the two-stream case considered above, the mean momentum $P_x$ oscillates at a constant frequency, the only difference being the amplitude of the oscillations (cf. Fig. 7).

https://doi.org/10.1017/S0022377803002101 Published online by Cambridge University Press

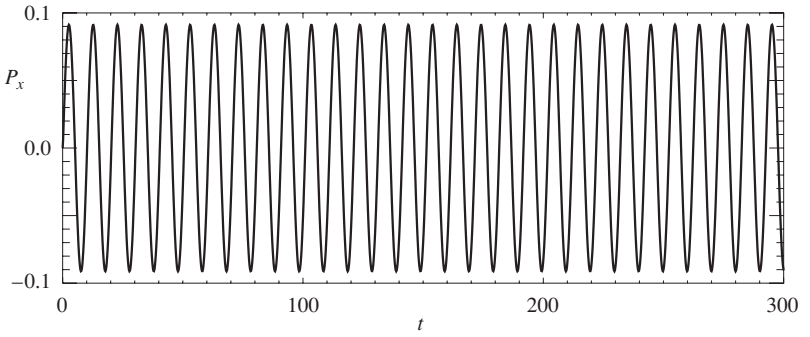


**Figure 7.** Oscillation of the total electron momentum in (3.3) during the development of phase space holes in Fig. 6.

## 5. Free plasma expansion

In order to gather some insight into the results of the previous two sections (notably the oscillations of the total electron momentum), in this section we attempt to reproduce phase space holes in a less conventional situation: free expansion of a plasma into vacuum. Since the Coulomb pull due to infinitely massive, cold ions would prevent electrons from expanding, in this section we consider *mobile ions*, for which the distribution $f_i(x, v_i, t)$ obeys the normalized Vlasov equation

$$\frac{\partial f_i}{\partial t} + v_i \frac{\partial f_i}{\partial x} + E \frac{\partial f_i}{\partial v_i} = 0, \tag{5.1}$$

subject to the same boundary condition of electrons

$$f_i(x = 0, v_i, t) = f_i(x = L, v_i, t) = 0. \tag{5.2}$$

Here and in the following the range of the ion velocity is $-v_{\max i} \leqslant v_i \leqslant v_{\max i}$, where $v_{\max i} = 0.28$ electrostatic units. Electrons obey (2.1), where the ion density is now given by $n_i(x,t) = \int_{-\infty}^{\infty} f_i(x, v_i, t)\, dv_i$, rather than by (2.2).

In the following both electrons and ions are initially in thermal equilibrium and distributed in velocity according to a Maxwellian; ions are initially homogeneous within the plateau $D < x < 3D$, whereas electrons are subject to an initial perturbation:

$$\left.\begin{aligned} f_e(x, v_e, t = 0) &= h_v(v_e)[1 + \varepsilon \cos(\alpha k_0 x)] \\ f_i(x, v_i, t = 0) &= (m_e/m_i)^{1/2} h_v((m_e/m_i)^{1/2} v_i) \end{aligned}\right\} \quad \text{for} \quad |x - 2D| < D,$$

$$f_e(x, v_e, t = 0) = f_i(x, v_i, t = 0) = 0 \quad \text{for} \quad |x - 2D| \geqslant D, \tag{5.3}$$

where $m_i$ is the ion mass.

For the simulation presented in Fig. 8, we choose $k_0 = 0.3, L = 32\pi/k_0, \varepsilon = 0.2, \alpha = \frac{3}{2}, m_i = 1837 m_e$; the electron and ion space and velocity coordinates $x$ and $v_e, v_i$ are discretized by the same number of points, $N_x = 2048$ and $N_v = 320$, respectively. The time step used in computation is $\Delta t = 0.1$, for both electrons and ions. For long-time behaviour and using a small (about 10) ion/electron mass ratio, such a problem was treated by Manfredi et al. (1993) and by Figua et al. (1999). However, in these works the appearance of the holes was hidden by a rescaling procedure used to deal with long-time evolution.

https://doi.org/10.1017/S0022377803002101 Published online by Cambridge University Press

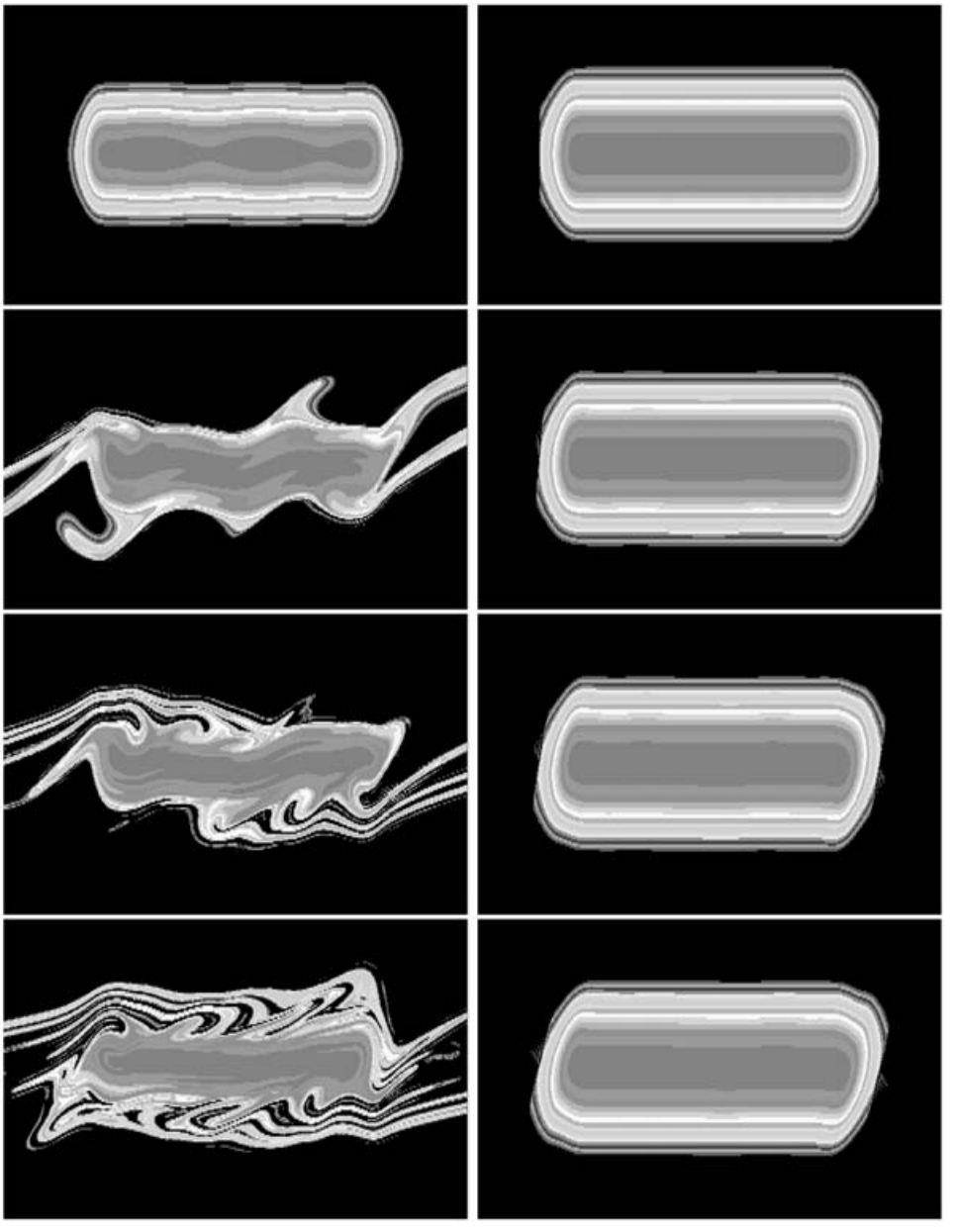

**Figure 8.** Evolution of the electron (left) and ions (right) distribution functions for the initial condition in (5.3) (free expansion of a plasma into vacuum), where $k_0 = 0.3, L = 32\pi/k_0$, $\varepsilon = 0.2, \alpha = \frac{3}{2}$, $m_i = 1837 m_e$. $N_x = 2048$, $N_v = 320$ points were used. Frame pairs, downward: $t = 0, 12, 24, 36$. Notice the build–up of filamentary structures in the plasma interfaces, close to the frames' borders. In all frames, only a restricted, central part of the phase space is shown: $0.48 \leqslant x/L \leqslant 0.52$; $-\frac{2}{3} \leqslant v_e/v_{\max e} \leqslant \frac{2}{3}$ for electrons, $-1 \leqslant v_i/v_{\max i} \leqslant 1$ for ions.

https://doi.org/10.1017/S0022377803002101 Published online by Cambridge University Press

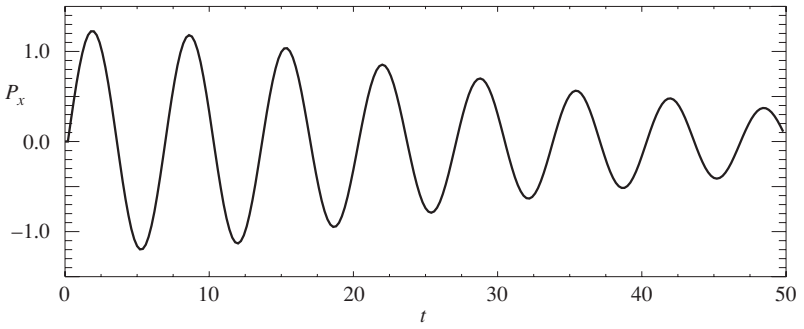


**Figure 9.** Oscillation of the total electron momentum in (3.3) during the development of phase space holes in Fig. 8. Notice the attenuation of the oscillations, at variance with Figs 4 and 7.

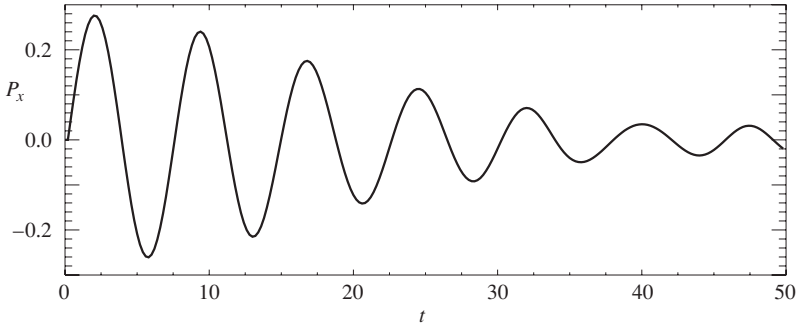


**Figure 10.** Same as in Fig. 9, but for $\varepsilon = 0.05$. Note decreasing the amplitude and frequency of the oscillations as compared with Fig. 9.

The behaviour of the total momentum is now different from that given in Secs 3 and 4: the frequency of the oscillations changes and their amplitude decreases in time, as the electrons expand into free space (cf. Fig. 9). Furthermore, simulating the expansion with a smaller perturbation leads to another important difference: not only does the oscillation amplitude decrease, but also its frequency turns out to be smaller than before (cf. Fig. 10).

## 6. Momentum oscillations

The oscillations of the total momentum in Figs 4 and 7 are a challenging task for theory to explain: they cannot be related to the above-mentioned cyclic revolution of holes in phase space: indeed, in Figs 3 and 6 we see that, for every positive contribution to the total momentum, due to rightward-moving electrons, there is a negative contribution, due to leftward-moving electrons which cancel the former contribution. A second way of thinking is that the oscillations of Figs 4 and 7 are due to perturbations of the plasma equilibrium. The nature of such an equilibrium is doubtless very complicated: contrary to the case of a spatially homogeneous plasma with periodic boundary conditions, holes do not reduce to a BGK state. The study of their stability in the fully kinetic regime, as performed for periodic

https://doi.org/10.1017/S0022377803002101 Published online by Cambridge University Press

boundary conditions (e.g. Schwarzmeier 1979), falls outside the scope of the present paper.

To simplify the situation we note that our equilibrium is formed by an inhomogeneous Maxwellian background on which the electrostatic component (holes) is superimposed. We assume that the latter is not important in determining the oscillation frequencies of the perturbations: in so doing we are supported by the fact that the equilibria in Figs 3 and 6 (which have the same Maxwellian background, but different hole configurations) have almost the same frequency of oscillation as shown in Figs 4 and 7, respectively. To further simplify the situation we adopt a fluid approach, since the quantity $P_x$ we are investigating is itself a fluid quantity. Also, in view of the mainly Maxwellian nature of the equilibrium, we can assume a vanishing heat flux (e.g. Boyd and Sanderson 1969), i.e. an adiabatic closure law. As a last simplification, in view of the harmonic nature of the oscillations of $P_x$, we use a linear theory. It is thus easy to reduce Vlasov's moment hierarchy to the following equation for the momentum density $p_x(x,t) = \int_{-\infty}^{\infty} v_e f_e(x, v_e, t)\, dv_e$:

$$\frac{\partial^2}{\partial t^2} p_x - \gamma \frac{\partial}{\partial x}\left(\frac{1}{n_i}\frac{\partial}{\partial x} p_x\right) = 0, \tag{6.1}$$

where $\gamma = \frac{5}{3}$ is the adiabatic exponent for the electron gas and $n_i(x)$ is the inhomogeneous background density given in (2.2) and in Fig. 1. We remind the reader that in (6.1) all electrostatic terms have been neglected, which reduces the normal modes of this equation to *electron sound waves*. Such normal modes can be written in the form $p_x(x,t) = q_x(x)\exp(-i\omega t)$ and the following equation and boundary conditions hold:

$$\omega^2 q_x + \gamma \frac{\partial}{\partial x}\left(\frac{1}{n_i}\frac{\partial}{\partial x} q_x\right) = 0, \quad q_x(0) = q_x(L) = 0. \tag{6.2}$$

With reference to Fig. 1, (6.2) is first solved in the interval $0 \leqslant x < D - 2d$ ($n_i = 0$, $q_x = 0$) and then in the interval $D - 2d \leqslant x \leqslant D$ ($n_i$ is the Epstein profile and $q_x$ is the hypergeometric series), by matching $q_x$ and its derivative at $x = D - 2d$. As a result of this procedure a value $q_x(D)$ is found. Now we notice that, in order to gather a non-vanishing total momentum $P_x(t) = \int_0^L p_x(x,t)\, dx$, we must consider only even solutions of (6.2) with respect to the point $x = 2D$ (cf. Fig. 1). The way to ensure this is to apply the same procedure used in the interval $0 \leqslant x \leqslant D$ to the interval $3D \leqslant x \leqslant L$; as a result, the same value of $q_x(D)$ will be found at $x = 3D$.

Finally, we integrate (6.2) in the interval $D < x < 3D$, where $n_i = 1$; the solution satisfying the symmetry condition and the boundary conditions $q_x(D) = q_x(3D)$ is

$$q_x(x) = q_x(D)\cos(\lambda x), \quad \omega = \gamma^{1/2}\lambda. \tag{6.3}$$

To compare the frequency $\omega$ with the results of the simulations we argue that the wavenumber $\lambda$ is the same as that of the initial perturbation: $\lambda = \alpha k_0$. Thus, in the case of the simulation of Sec. 3 ($\alpha = \frac{3}{2}, k_0 = 0.3$) we obtain a period for the oscillation $T = 2\pi/\omega = 10.82$; for the simulation of Sec. 4 ($\alpha = 1, k_0 = 0.427\,12$) we obtain $T = 2\pi/\omega = 11.32$. Such values are in good agreement with the results in Fig. 4 ($T \simeq 10$) and Fig. 7 ($T \simeq 10$), respectively.

We notice that, on calculating $P_x = \int_0^L q_x(x)\, dx$, the contribution coming from the central plateau ($D < x < 3D$) averages to zero, due to periodicity of $q_x$, but the contribution coming from the interfaces ($D - 2d \leqslant x \leqslant D$ and $3D \leqslant x \leqslant 3D + 2d$)

https://doi.org/10.1017/S0022377803002101 Published online by Cambridge University Press

is generally non-zero. We conclude that the observed oscillation of $P_x$ *owe their existence to the interfaces*, and thus they vanish if the background plasma is strictly homogeneous.

We now come to Sec. 5 and to Figs 9 and 10 in which the wavenumber of the initial perturbations is $\alpha k_0 = 0.45$; for such a value the frequency of Langmuir waves is about 1.35 and its Landau damping rate would be about 0.11 (Canosa 1973): such values are noticeably different from those observed in Figs 9 and 10. It is thus unlikely that the oscillations observed are due to Landau-damped Langmuir waves. Nevertheless, we have to explain how an apparent attenuation can occur in our otherwise non-dissipative system.

To do so, let us attempt a fluid interpretation of the attenuated oscillations of Figs 9 and 10. We expect (Sack and Schamel 1987) that, as the plasma expands, the width of the interfaces $2d$ increase. In the limiting case, as $d \to \infty$, we would have no interface at all and, as noted above, the oscillations of the total momentum should vanish; this is in qualitative agreement with what is shown in Figs 9 and 10. More specifically, rewrite (6.2) as

$$\frac{\partial^2}{\partial s^2} q_x + \frac{\omega^2}{\gamma} \frac{1}{n_i} q_x = 0, \tag{6.4}$$

where $s = \int n_i(x)\, dx$ is a monotonically increasing function of $x$ in the interface $D - 2d \leqslant x \leqslant D$. Since, due to conservation of total mass, $n_i$ decreases as the plasma occupies larger and larger volumes of space, then, according to (6.4), the curvature of $q_x$ increases to the stage that the gradients of $q_x$ will become much steeper than the gradients of $n_i$, which can thus be regarded as a constant. This leads to a sinusoidal solution of (6.4), possessing a larger and larger wavenumber as the plasma expands: in this way the distribution function develops the filamentary structures which are indeed observed in Fig. 8. Since such a sinusoidal solution averages to a smaller and smaller value as its 'corrugation' increases, it is easy to see that the contribution to the total momentum provided by the interface is attenuated, as indeed shown in Figs 9 and 10.

It is thus shown that the attenuation is just an instance of *phase mixing* and it can occur even in our non-dissipative system, in the same way as it does for Landau damping, for which 'corrugation' occurs in the velocity space (Sedláček 1995).

## 7. Conclusions

In this article we studied the effect of *non-periodic boundary conditions* on the development of holes in the phase space of a non-collisional, hot plasma governed by the Vlasov–Poisson system of equations. Four situations were considered through the prescription of four different initial conditions: (a) development of a sinusoidal wave; (b) development of the two-stream instability; (c) development of an *ab initio* BGK state; (d) free expansion of the plasma into vacuum. In cases (a)–(c) ions were kept immobile; in case (d) they move with a realistic mass of 1837 electron masses.

In situations (a)–(c) the development of the plasma subject to periodic boundary conditions was extensively investigated in the literature and it is fairly well understood: holes appear in phase space which may have both a vanishing mean velocity (e.g. case c) and a non-vanishing mean velocity (e.g. case b). The former may sometimes coalesce into a single hole, a phenomenon which also took place under the non-periodic boundary conditions of our present investigation.

https://doi.org/10.1017/S0022377803002101 Published online by Cambridge University Press

On the other hand, under periodic boundary conditions, non-vanishing velocity holes move at a constant speed along the space coordinate: they leave the computational box on one side and re-enter it from the other side. Since this possibility is prevented under the non-periodic boundary conditions used in our present work (cf. 2.3 and 5.2), the question arises at to what is the fate of these holes as they approach the plasma boundaries.

Our investigation reveals that approaching the right boundary, positive mean velocity holes *'turn' clockwise* and move along the velocity coordinate: they are first decelerated, then accelerated to acquire a negative velocity (thus becoming negative mean velocity holes) and then turn clockwise again (thus reversing their original sense of motion). When they reach the left boundary, again they turn clockwise, are decelerated and then accelerated to acquire a positive velocity (thus becoming positive mean velocity holes again). This fact results in a periodic revolution of holes in phase space.

A second major result of our investigation is the appearance of time oscillations of the total electron momentum $P_x$ (cf. 3.3) over the electron time scale. For immobile ions these oscillations have a remarkably periodic behaviour (cf. Figs 4 and 7); on the other hand, for mobile ions, the plasma expands into vacuum and the oscillations are attenuated in time (cf. Figs 9 and 10). We proved that these oscillations are related neither to electrostatic holes nor to electron plasma waves.

Rather, by means of a simplified model, we showed that the oscillations are due to *electron sound waves* caused by the same initial perturbations leading to electrostatic holes; these waves are trapped in the plasma interfaces and they are attenuated during plasma expansion, as sound waves phase-mix in the wider and wider expanding interfaces. The fact that, for all the cases studied in this paper, these oscillations never grow in time is an encouraging result in favour of the stability of the electrostatic hole structures.

*Acknowledgements*

This work was supported by the Centre National de la Recherche Scientifique and by Consiglio Nazionale delle Ricerche. The authors are also grateful to the Centre International d'Ateliers Scientifiques for supporting the workshop 'Space plasma phenomena at the collisional/noncollisional interplay' in June 2001, where this investigation was initiated.

## References

Armstrong, T. P. and Montgomery, D. 1969 Numerical study of weakly unstable electron plasma oscillations. *J. Plasma Phys.* **1**, 2094–2098.

Berk, H. L. and Roberts, K. V. 1967 Nonlinear study of Vlasov's equation for a special class of distribution functions. *Phys. Fluids* **10**, 1595–1597.

Berk, H. L., Nielsen, C. E. and Roberts, K. V. 1970 Phase space hydrodynamics of equivalent nonlinear systems: experimental and computational observations. *Phys. Fluids* **13**, 980–995.

Berman, R. H., Dupree, T. H. and Tetreault, D. J. 1986 Growth of nonlinear intermittent fluctuations in linearly stable and unstable simulation plasma. *Phys. Fluids* **29**, 2860–2870.

Bernstein, I. B. 1958 Waves in a plasma in a magnetic field. *Phys. Rev.* **109**, 10–20.

Bertrand, P., Ghizzo, A., Feix, M. R., Fijalkow, E., Mineau, P., Suh, N. D. and Shoucri, M. 1989. In *Non linear Vlasov plasmas* (ed. F. Doveil). Orsay: Les éditions de Physique, p. 109.

Boutros-Ghali, T. and Dupree, T. H. 1981 Theory of two-point correlation function in a Vlasov plasma. *Phys. Fluids* **24**, 1839–1858.

Boyd, T. J. M. and Sanderson, J. J. 1969 *Plasma Dynamics*. London: Nelson.

Brunetti, M., Califano, F. and Pegoraro, F. 2000 Asymptotic evolution of nonlinear Landau damping. *Phys. Rev. Lett.* **62**, 4109–4114.

Canosa, J. 1973 Numerical solution of Landau's dispersion relation. *J. Comp. Phys.* **13**, 158–160.

Chanteur, G. and Raadu, M. 1987 Formation of shocklike modified Korteweg–de Vries solitons: application to double layers. *Phys. Fluids* **30**, 2708–2719.

Dupree, T. H. 1982 Theory of phase space density holes. *Phys. Fluids* **25**, 277–289.

Fijalkow, E. 1999 Behaviour of phase space holes in 2D simulations. *J. Plasma Phys.* **61**, 65–76.

Figua, H., Garcia, L. G., Fijalkow, E. and Goedert, J. 1999 Expansion of a negative ion plasma into vacuum. In *Dynamical Systems, Plasmas and Gravitation* (eds. P. G. L. Leach, S. E. Bouquet, J. L. Rouet and E. Fijalkow). Berlin: Springer, pp. 62–73.

Ghizzo, A., Izrar, B., Bertrand, P., Fijalkow, E., Feix, M. R. and Shoucri, M. 1988 Stability of Bernstein–Green–Kruskal plasma equilibria. Numerical experiments over a long time. *Phys. Fluids* **31**, 72–82.

Han, J. M. and Kim, K. Y. 1995 Dynamics of non-monotonic double layers. *J. Phys. Soc. Japan* **64**, 1172–1185.

Hasegawa, A. and Sato, T. 1982 Existence of a negative potential solitary-wave structure and formation of a double layer. *Phys. Fluids* **25**, 632–635.

Klimas, A. J. and Farrell, W. M. 1994 Splitting algorithm for Vlasov simulation with filamentation filtration. *J. Comp. Phys.* **110**, 150–163.

Korn, J. and Schamel, H. 1996 Electron holes and their role in the dynamics of current-carrying weakly collisional plasmas. Part 1. Immobile ions. *J. Plasma Phys.* **56**, 307–337.

Manfredi, G. 1997 Long-time behaviour of nonlinear Landau damping. *Phys. Rev. Lett.* **79**, 2815–2818.

Manfredi, G., Mola, S. and Feix, M. R. 1993 Rescaling methods and plasma expansions into vacuum. *Phys. Fluids* **B5**, 388–401.

Mineau, P. 1989 Resolution numerique du systeme Vlasov–Poisson. Application a des problemes de l'Astrophysique et de la Physique des plasmas. *PhD thesis*, Université d'Orléans, Part 1, chapter II.

Muschietti, L., Roth, I., Ergun, R. E. and Carlson, C. W. 1999 Analysis and simulations of BGK electron holes. *Nonlinear Process. Geophys.* **6**, 211–219.

Nocera, L. and Mangeney, A. 1999 Evidence for second order oscillations at the Best frequency in direct numerical simulations of the Vlasov equation. *Phys. Plasmas* **6**, 4559–4564.

Oppenheim, M. M., Vetoulis, G., Newman, D. L. and Goldman, M. V. 2001 Evolution of electron phase space holes in 3D. *Geophys. Res. Lett.* **28**, 1891–1894.

Roberts, K. V. and Berk, H. L. 1967 Nonlinear evolution of a two-stream Instability. *Phys. Rev. Lett.* **101**, 297–300.

Sack, Ch. and Schamel H. 1987 Plasma expansion into vacuum – a hydrodynamic approach. *Phys. Rep.* **156**, 311–395.

Saeki, K. and Genma, H. 1998 Electron–hole disruption due to ion motion and formation of coupled electron–hole and ion-acoustic soliton plasma. *Phys. Rev. Lett.* **80**, 1224–1227.

Sato, T. and Okuda, H. 1980 Ion-acoustic double layers. *Phys. Plasmas* **2**, 740–743.

Schamel, H. 1982 Kinetic theory of phase space vortices and double layers. *Physica Scripta* **T2/1**, 228–237.

Schamel, H. 1986 Electron holes, ion holes and double layers. *Phys. Rep.* **40**, 161–191.

Schamel, H. 2000 Hole equilibria in Vlasov–Poisson systems: a challenge to wave theories of ideal plasmas. *Plasma Phys.* **7**, 4831–4844.

Schwarzmeier, J. L. 1979 Stability of Bernstein–Greene–Kruskal equilibria. *Phys. Fluids* **29**, 1747–1760.

Sedláček, Z. 1995 Continuum damping in plasma physics. In *Proc. 1994 Int. Conf. on Plasma Physics* (eds. P. H. Sakanaka and M. Tendler). Woodbury, NY: AIP Press, p. 119.

Shoucri, M. M. and Gagne, R. R. J. 1978 Splitting schemes for the numerical solution of a two-dimensional Vlasov equation. *J. Comp. Phys.* **27**, 315–322.

Singh, N., Loo, S. M., Wells, B. E. and Deverapalli, C. 2000 Three-dimensional structure of electron holes driven by an electron beam. *Geophys. Res. Lett.* **27**, 2469–2472.

Terry, P. W., Diamond, P. H. and Hahm, J. D. 1990 The structure and dynamics of electrostatic and magnetostatic drift holes. *Phys. Fluids* **B2**, 2048–2063.